PHYSICAL REVIEW D VOLUME 15, NUMBER 4 15 FEBRUARY 1977

Strong-coupling calculations of the hadron spectrum of quantum chromodynamics

T. Banks,* S. Raby,* and L. Susskind*†
Tel Aviv University, Ramat Aviv, Israel

J. Kogut*‡
Laboratory of Nuclear Studies, Cornell University, Ithaca, New York 14853

D. R. T. Jones,§ P. N. Scharbach,§ and D. K. Sinclair‖
Department of Theoretical Physics, University of Oxford, Oxford 0X1-3PQ, England
(Received 13 August 1976)

We present calculations of the low-energy mass spectrum and matrix elements of quantum chromodynamics. We employ an isospin doublet of massless quarks and analyze the theory from the strong-coupling limit using a particularly simple lattice Hamiltonian. In the strong-coupling limit the vacuum state has exact local color symmetry, but spontaneously breaks those elements of chiral symmetry which are present in the lattice Hamiltonian. Expansions for masses (π, ρ, ω, σ, A_1, B, f, and nucleon) and matrix elements (g_A) in the reciprocal coupling constant are analytically continued to the continuum limit using Padé approximants. The results are in surprisingly good agreement with experiment except for the pion mass. This single failure is traced to the lack of full chiral symmetry in the theory for large lattice spacing and the lack of significant spin-spin forces in low orders of strong-coupling perturbation theory. Higher-order calculations should resolve this problem, but a more realistic Hamiltonian suggested by renormalization-group analyses also looks promising.

I. INTRODUCTION

Quantum chromodynamics[1] is a promising candidate for the theory of strong interactions. The theory consists of several flavors of colored quarks which interact with flavor-neutral colored Yang-Mills gluons in a locally color-gauge-invariant fashion. The short-distance properties of the theory are computable since the theory's invariant charge vanishes at short distances.[2] In addition, there are reasons to believe that the theory is strongly coupled at large distances in such a way that its low-energy spectrum consists of only color-singlet hadrons.[3] The hope is that the spectrum of these field-theoretic bound states reproduces the Rosenfeld tables. This paper addresses the strong-coupling problem and it reports results on low-order calculations of the theory's spectrum in a particularly simple lattice formulation of the theory. Many of the results reported here are quite realistic and encouraging, but considerable work remains to be done.

In order to calculate masses and matrix elements of a field theory which is strongly coupled at large distances we follow Wilson[4] and Polyakov[5] (as interpreted by Kogut and Susskind[6]), and quantize the theory on a discrete spatial lattice. This method has been applied successfully to QED in $1+1$ dimensions[7] and to the non-Abelian Thirring model.[8] The application of these methods to $(3+1)$-dimensional theories has been previously illustrated for a pure Yang-Mills field theory.[9]

In this paper we couple an isodoublet of massless colored quarks to the Yang-Mills fields and calculate various meson and baryon masses and matrix elements. We choose to restrict ourselves to the SU(2) flavor group for several reasons. First, we are interested in the lowest-lying part of the hadron spectrum. Heavy quarks are not expected to be important here. In addition, the success of current-algebra sum rules and partial conservation of axial-vector current (PCAC) strongly suggest that chiral symmetry is spontaneously broken and the pion appears as a Goldstone boson of strong interactions. It remains an important challenge to theorists to see if this physical picture can be obtained explicitly from a field theory employing only quarks and gluons. This challenge motivates our choice of degrees of freedom and our lattice-fermion technique in which the absence of a mechanical quark mass follows from a natural symmetry of the lattice theory (discrete chiral symmetry in this case).

Our calculations begin with a consideration of the ground state for large coupling, $g \gg 1$. The ground state is found to be gauge invariant. No Higgs phenomenon[10] occurs. This indicates that there is quark confinement on the lattice for large g.[6] Chiral symmetry is spontaneously broken via a nonzero vacuum expectation value of $\bar{q}q$ (q is the quark field).

Next we consider the masses of the $\pi, \rho, \omega, \sigma, f_2, B, A_1$, nucleon and the nucleon's axial-vector charge g_A. In the strong-coupling limit the zeroth-

order meson-nucleon mass ratios are all equal and have the value

$$m^{(0)}_{\text{meson}}/m^{(0)}_{\text{nucleon}} = 1.25 \tag{1.1}$$

for a convenient choice of an irrelevant parameter A (see later). In the same limit the nucleon's axial-vector charge is

$$g_A^{(0)} = 3.00 \ . \tag{1.2}$$

We next perturb in the parameter $x \equiv 1/g^2$ in the strong-coupling limit and extrapolate to the continuum limit [lattice spacing $a \to 0$, $g(a) \to 0$] using Padé approximants. Through fourth order in x we find, for our mass ratios,

$$\begin{aligned}
&m_\rho^{(4)}/m_N^{(4)} = 0.822 \ (0.820) \ , \\
&m_\omega^{(4)}/m_N^{(4)} = 0.824 \ (0.834) \ , \\
&m_\pi^{(4)}/m_N^{(4)} = 0.820 \ (0.147) \ , \\
&m_\sigma^{(4)}/m_N^{(4)} = 0.972 \ (0.820\text{–}1.10, \text{ broad}) \ , \\
&m_B^{(4)}/m_N^{(4)} = 1.05 \ (1.32) \ , \\
&m_f^{(4)}/m_N^{(4)} = 1.17 \ (1.35) \ , \\
&m_{A_1}^{(4)}/m_N^{(4)} = 1.12 \ (1.17) \ ,
\end{aligned} \tag{1.3}$$

while the fourth-order axial-vector charge is

$$g_A^{(4)} = 1.81 \ (1.24) \ . \tag{1.4}$$

The experimental values for these quantities are the numbers listed above in parentheses.

With the exception of the pion, the fourth-order results for the mass spectrum are very encouraging. The fourth-order mass ratios are substantially more realistic than the zeroth-order static values; all the p-wave mesons are more massive than the s-wave mesons and the magnitudes of the splittings are quite realistic. It is also true that the fourth-order results are *not* sensitive to the zeroth-order mass ratios whose values depend on the details of the lattice Hamiltonian. This is an important indication that our method for extracting approximate continuum physics from the lattice formulation of the theory is basically sound.

A particularly interesting feature of these calculations is that the mass ratios of Eq. (1.3) and the dimensionless matrix element g_A are *free of any* parameters. This fact is a consequence of the asymptotic freedom[2] of the continuum field theory and the absence of any explicit mass scale in the continuum Hamiltonian. It comes about in the lattice theory because the isodoublet of quarks are massless to all orders of perturbation theory, and the bare coupling constant $g(a)$ vanishes in the continuum limit $a \to 0$. Once higher-order calculations are complete, the quantities of Eq. (1.3) and (1.4) will, we hope approach the experimental numbers to within several percent. In principle, the accuracy of the method is limited only by our neglect of electromagnetic effects, heavy quarks, explicit chiral-symmetry breaking, etc.

Clearly the most notable failure of the fourth-order calculations is the pion mass which, because of our approximation of zero quark mass and the spontaneous breakdown of chiral symmetry, should be zero. We are confident that the pion mass will decrease as higher-order calculations are completed. Since the strong-coupling perturbation-theory methods used here are simple and systematic, high-order computer calculations are in progress.[11] At least two more orders in the strong-coupling expansions will be available in the near future. A survey of graphs indicates the possibility of substantial π-ρ splitting in sixth- and eighth-order expansion coefficients. It will be interesting to see whether the good results of Eqs. (1.3) and (1.4) will also improve in higher orders while the π-ρ splitting becomes realistic.

This article is organized into seven sections. In Sec. II we review the lattice-fermion method introduced by one of us.[12] In Sec. III the theory's vacuum for large g is explored. We find that it is locally color-gauge invariant but spontaneously breaks a natural symmetry of the lattice Hamiltonian, discrete chiral transformations. One's freedom to add irrelevant operators to the Hamiltonian without affecting the physics of the continuum limit is discussed. The fourth-order calculation of the vacuum energy is illustrated in detail. In Sec. IV the wave functions of the mesons and nucleon are obtained, second-order calculations of their energies are illustrated, and fourth-order results are recorded. Section V discusses mass ratios in the continuum limit and contains fourth-order numerical results. The calculation of g_A appears in Sec. VI. The article closes with a discussion of results and directions for future work in Sec. VII. Hamiltonian calculations employing the wisdom of Wilson's block spin analyses[13] are briefly mentioned.

II. LATTICE QUANTUM CHROMODYNAMICS

First let us review the Susskind approach[12] to nonstrange quarks on a lattice. One can show that it is possible to represent the two nonstrange quark fields u and d by a single-component lattice field $\chi(\vec{r})$. The χ's obey the canonical anticommutation relations

$$\begin{aligned}
&\{\chi(\vec{r}), \chi^\dagger(\vec{r}\,')\} = \delta_{\vec{r},\vec{r}'} \ , \\
&\{\chi(\vec{r}), \chi(\vec{r}')\} = 0 \ .
\end{aligned} \tag{2.1}$$

χ carries a conventional color index but no spinor or isospinor indices. The lattice sites are labeled by a triplet of integers $\vec{r} = (x, y, z)$. A dimensional

lattice spacing a is required to connect ordinary "laboratory" units with lattice units.

For the case of free, massless quarks the lattice Hamiltonian is

$$H_{\text{quark}}=\frac{1}{2a}\sum_{\vec{r}}[\chi^{\dagger}(\vec{r})\chi(\vec{r}+\hat{z})(-1)^{y}+\chi^{\dagger}(\vec{r})\chi(\vec{r}+\hat{x})(-1)^{z}+\chi^{\dagger}(\vec{r})\chi(\vec{r}+\hat{y})(-1)^{x}+\text{H.c.}], \quad (2.2)$$

or, using the notation

$$\eta(\hat{z})=(-1)^{y},\ \eta(\hat{x})=(-1)^{z},\ \eta(\hat{y})=(-1)^{x},\ \eta(-\hat{n})=\eta(\hat{n}), \quad (2.3)$$

we have

$$H_{\text{quark}}=\frac{1}{2a}\sum_{\vec{r},\hat{n}}\chi^{\dagger}(\vec{r})\chi(\vec{r}+\hat{n})\eta(\hat{n}), \quad (2.4)$$

where the sum is over the six directions $\hat{n}$.

To make the connection between χ and the conventional quark fields u and d, it is helpful to introduce an auxiliary field ϕ:

$$\phi(\vec{r})=\frac{(-1)^{x+y+z}}{2\sqrt{2}}(-i)^{z+x}[(i)^{y-1/2}+(-i)^{y-1/2}]\times[(-1)^{x}+(-1)^{z}-(-1)^{x+z}+1]\chi(\vec{r})\equiv S(\vec{r})\chi(\vec{r}). \quad (2.5)$$

Clearly $S(\vec{r})=\pm i$ on each site. Substituting Eq. (2.5) into Eq. (2.2) gives

$$H_{\text{quark}}=\frac{-i}{2a}\sum_{\vec{r}}\{[\phi^{\dagger}(\vec{r})\phi(\vec{r}+\hat{z})-\text{H.c.}](-1)^{x+y}+[\phi^{\dagger}(\vec{r})\phi(\vec{r}+\hat{x})-\text{H.c.}]+i[\phi^{\dagger}(\vec{r})\varphi(\vec{r}+\hat{y})+\text{H.c.}](-1)^{x+y}\}. \quad (2.6)$$

This gives the following equation of motion for ϕ:

$$\dot{\phi}(\vec{r})=\frac{-1}{2a}\{[\phi(\vec{r}+\hat{z})-\phi(\vec{r}-\hat{z})](-1)^{x+y}+[\phi(\vec{r}+\hat{x})-\phi(\vec{r}-\hat{x})]+i[\phi(\vec{r}+\hat{y})-\phi(\vec{r}-\hat{y})](-1)^{x+y}\}. \quad (2.7)$$

In momentum space let $\phi(\vec{k})$ $(-\pi\le k_i\le\pi, i=x,y,z)$ be the "Fourier transform" of $\phi(\vec{r})$. For any wave vector $\vec{k}$, define modulo 2π,

$$\begin{aligned}
&\vec{k}+\vec{\pi}_x=(k_x+\pi,k_y,k_z),\\
&\vec{k}+\vec{\pi}_y=(k_x,k_y+\pi,k_z),\\
&\vec{k}+\vec{\pi}_z=(k_x,k_y,k_z+\pi),\\
&\vec{k}+\vec{\pi}_{xy}=(\vec{k}+\vec{\pi}_x)+\vec{\pi}_y=(\vec{k}+\vec{\pi}_y)+\vec{\pi}_x,\\
&\vec{k}+\vec{\pi}_{yz}=(\vec{k}+\vec{\pi}_y)+\vec{\pi}_z,\\
&\vec{k}+\vec{\pi}_{xz}=(\vec{k}+\vec{\pi}_x)+\vec{\pi}_z,\\
&\vec{k}+\vec{\pi}_{xyz}=(\vec{k}+\vec{\pi}_{xy})+\vec{\pi}_z.
\end{aligned} \quad (2.8)$$

Now Eq. (2.7) becomes

$$\omega\phi(\vec{k})=\frac{\sin k_z}{a}\phi(\vec{k}+\vec{\pi}_{xy})+\frac{\sin k_x}{a}\phi(\vec{k})+i\frac{\sin k_y}{a}\phi(\vec{k}+\vec{\pi}_{xy}). \quad (2.9)$$

Now defining

$$\begin{aligned}
2u_1(\vec{k})&=\phi(\vec{k})+\phi(\vec{k}+\vec{\pi}_z)+\phi(\vec{k}+\vec{\pi}_{xy})+\phi(\vec{k}+\vec{\pi}_{xyz}),\\
2u_2(\vec{k})&=\phi(\vec{k})-\phi(\vec{k}+\vec{\pi}_z)-\phi(\vec{k}+\vec{\pi}_{xy})+\phi(\vec{k}+\vec{\pi}_{xyz}),\\
2u_3(\vec{k})&=\phi(\vec{k})-\phi(\vec{k}+\vec{\pi}_z)+\phi(\vec{k}+\vec{\pi}_{xy})-\phi(\vec{k}+\vec{\pi}_{xyz}),\\
2u_4(\vec{k})&=\phi(\vec{k})+\phi(\vec{k}+\vec{\pi}_z)-\phi(\vec{k}+\vec{\pi}_{xy})-\phi(\vec{k}+\vec{\pi}_{xyz}),
\end{aligned} \quad (2.10)$$

$$\begin{aligned}
2d_1(\vec{k})&=-\phi(\vec{k}+\vec{\pi}_x)+\phi(\vec{k}+\vec{\pi}_y)-\phi(\vec{k}+\vec{\pi}_{yz})+\phi(\vec{k}+\vec{\pi}_{xz}),\\
2d_2(\vec{k})&=-\phi(\vec{k}+\vec{\pi}_x)-\phi(\vec{k}+\vec{\pi}_y)-\phi(\vec{k}+\vec{\pi}_{yz})-\phi(\vec{k}+\vec{\pi}_{xz}),\\
2d_3(\vec{k})&=\phi(\vec{k}+\vec{\pi}_x)-\phi(\vec{k}+\vec{\pi}_y)-\phi(\vec{k}+\vec{\pi}_{yz})+\phi(\vec{k}+\vec{\pi}_{xz}),\\
2d_4(\vec{k})&=\phi(\vec{k}+\vec{\pi}_x)+\phi(\vec{k}+\vec{\pi}_y)-\phi(\vec{k}+\vec{\pi}_{yz})-\phi(\vec{k}+\vec{\pi}_{xz}),
\end{aligned}$$

then Eq. (2.9) is equivalent to

$$\begin{aligned}
\omega u_1(\vec{k})&=\frac{\sin k_z}{a}u_3+\frac{\sin k_x}{a}u_4-i\frac{\sin k_y}{a}u_4,\\
\omega u_2(\vec{k})&=-\frac{\sin k_z}{a}u_4+\frac{\sin k_x}{a}u_3+i\frac{\sin k_y}{a}u_3,\\
\omega u_3(\vec{k})&=\frac{\sin k_z}{a}u_1+\frac{\sin k_x}{a}u_2-i\frac{\sin k_y}{a}u_2,\\
\omega u_4(\vec{k})&=-\frac{\sin k_z}{a}u_2+\frac{\sin k_x}{a}u_1+i\frac{\sin k_y}{a}u_1,
\end{aligned} \quad (2.11)$$

and identical equations for the d's.

Evidently if ω is to remain finite as $a\to 0$ we must require each component of $\vec{k}$ to be near 0 or π. More precisely,

$$\vec{k}-\vec{\pi}_i=a\vec{K},\quad i\in[1,8], \quad (2.12)$$

where $\vec{K}$ remains finite as $a\to 0$.

Let us consider those normal modes with $\vec{k}$ small. Specifically set $\vec{k}=a\vec{K}$. Equation (2.11) for small a takes the form

$$\begin{aligned}
\omega u_1(\vec{K})&=K_z u_3+K_x u_4-iK_y u_4,\\
\omega u_2(\vec{K})&=-K_z u_4+K_x u_3+iK_y u_4,\\
\omega u_3(\vec{K})&=K_z u_1+K_x u_2-iK_y u_2,\\
\omega u_4(\vec{K})&=-K_z u_2+K_x u_1+iK_y u_1,
\end{aligned} \quad (2.13)$$

and the same with $u\leftrightarrow d$.

These are the normal Dirac equations for u and d in the representation

$$\gamma_0=\begin{pmatrix}1&0\\0&-1\end{pmatrix},\quad \vec{\alpha}=\begin{pmatrix}0&\vec{\sigma}\\\vec{\sigma}&0\end{pmatrix}. \quad (2.14)$$

The set of normal modes satisfying Eq. (2.13) are complete for

$$-\frac{\pi}{2} \leq k_{x,y,z} < \frac{\pi}{2} . \tag{2.15}$$

In fact, the eight fields $u_i(\vec{k})$ and $d_i(\vec{k})$ for $\vec{k}$ restricted by Eq. (2.15) replace $\phi(\vec{k})$ on the interval

$$-\pi \leq k_{x,y,z} \leq \pi . \tag{2.16}$$

Hence for finite-energy modes, our system describes an *isodoublet* of massless quark fields.

We now examine the symmetries of the theory, working in the χ representation where they can most easily be seen. They are as follows:

(*a*) *Lattice translation by even integers*,

$$\chi(x,y,z) \to \chi(x+2l, y+2m, z+2n), \tag{2.17}$$

with l, m, and n integers. This is identified as discrete translation invariance.

(*b*) *Lattice translation by a single link*,

$$\begin{aligned} &\chi(\vec{r}) \to \chi(\vec{r} \pm \hat{x})(-1)^y , \\ &\chi(\vec{r}) \to \chi(\vec{r} \pm \hat{y})(-1)^z , \\ \text{or} \quad &\chi(\vec{r}) \to \chi(\vec{r} \pm \hat{z})(-1)^x . \end{aligned} \tag{2.18}$$

In momentum space we see that the last of these can be written as

$$q \to e^{ik_z} \gamma_5 \tau_3 q . \tag{2.19}$$

In the continuum limit where k_z is infinitesimal, this becomes

$$q \to \gamma_5 \tau_3 q , \tag{2.20a}$$

while the other two transformations become

$$q \to \gamma_5 \tau_2 q \tag{2.20b}$$

and

$$q \to \gamma_5 \tau_1 q , \tag{2.20c}$$

This discrete chiral invariance is an extremely important feature of our formalism. Without it we would have no control over induced (divergent) quark masses when interactions are turned on. At the present time there it no other formalism which satisfies this requirement and which is simple enough to use in strong-coupling calculations.

(*c*) *Shift along a "face" diagonal*,

$$\begin{aligned} &\chi(\vec{r}) \to (-1)^{x+y} \chi(\vec{r} + \hat{x} + \hat{z}) , \\ &\chi(\vec{r}) \to (-1)^{y+z} \chi(\vec{r} + \hat{y} + \hat{x}) , \\ \text{or} \quad &\chi(\vec{r}) \to (-1)^{z+x} \chi(\vec{r} + \hat{z} + \hat{y}) , \end{aligned} \tag{2.21}$$

which define the discrete isospin rotations

$$\begin{aligned} &q \to \tau_2 q , \\ &q \to \tau_3 q , \\ &q \to \tau_1 q . \end{aligned} \tag{2.22}$$

(*d*) *Cubic lattice rotation*. These rotate the lattice by $\pi/2$ about any axis keeping one site, $x=y=z=0$ say, fixed. If $\vec{r} \to \vec{r}'$ is such a rotation, then χ transforms thus

$$\begin{aligned} \chi(\vec{r}) &\to \tfrac{1}{2}[(-1)^y + (-1)^z + (-1)^x - (-1)^{x+y+z}] \chi(\vec{r}') \\ &\equiv R(x,y,z) \chi(\vec{r}') . \end{aligned} \tag{2.23}$$

These transformations are not identified as spatial rotations by $\pi/2$ of the quark fields, but simultaneous space and isospin rotations by $\pi/4$, viz.,

$$\begin{aligned} &q(\vec{r}) \to \exp\left[i \frac{\pi}{4} (\sigma_x + \tau_1)\right] q(\vec{r}') , \\ &q(\vec{r}) \to \exp\left[i \frac{\pi}{4} (\sigma_y + \tau_2)\right] q(\vec{r}') , \\ &q(\vec{r}) \to \exp\left[i \frac{\pi}{4} (\sigma_z + \tau_3)\right] q(\vec{r}') \end{aligned} \tag{2.24}$$

for rotations about the x, y, and z axes, respectively.

(*e*) *Rotations by π about a body center*. These are rotations about the geometrical center of a given lattice cube about any of the three axes and they represent ordinary spatial rotations by π.

(*f*) *Parity*. This is simply reflection through the origin

$$\chi(\vec{r}) \to \chi(-\vec{r}) . \tag{2.25}$$

(*g*) *G parity*. This is just complex conjugation

$$\chi(\vec{r}) \to \chi^\dagger(\vec{r}) . \tag{2.26}$$

The symmetries (a)–(g) are not *a priori* sufficient to guarantee continuous isospin and rotational invariance in the long-wavelength behavior of an interacting theory. However, if the dimensionless couplings are small, any asymmetries must manifest themselves as induced renormalizable or superrenormalizable counterterms. In our case there are no such terms consistent with the discrete symmetries of the lattice theory. For example, a quark mass term is superrenormalizable, but it is not invariant under the discrete chiral transformation $q \to \tau_i \gamma_5 q$. Therefore, if the bare lattice Hamiltonian is written for massless quarks, the quarks will remain massless order by order in perturbation theory. This fact is the central motivation for the lattice-fermion method discussed here.

Now consider the introduction of the gauge fields. Following Refs. 4–6 the gauge field is defined on the links of the lattice. We restrict ourselves to that limited class of gauges for which $\vec{A}^0 \equiv 0$.[6] A

directed link is specified by a site $\vec{r}$ and a unit vector $\hat{n}$. Each site is the origin of six directed links, and each pair of neighboring sites define two directed links. For each link a degree of freedom $U(\vec{r},\hat{n})$ is defined. U is a matrix of the fundamental representation of the SU(3) color group. The two gauge fields occupying the "same" link are related by

$$U(\vec{r},\hat{n})=U^{\dagger}(\vec{r}+\hat{n},-\hat{n})\,. \tag{2.27}$$

In terms of the more familiar gauge field $\vec{A}^{i}$,

$$U(\vec{r},\hat{n})=\exp(igaA^{i}_{\alpha}\lambda^{\alpha}\hat{n}^{i}/2)\,. \tag{2.28}$$

The gauge-invariant form of the quark Hamiltonian is now

$$H_{q}=\frac{1}{2a}\sum_{\vec{r},\hat{n}}\chi^{\dagger}(\vec{r})U(\vec{r},\hat{n})\chi(\vec{r}+\hat{n})\eta(\hat{n})\,, \tag{2.29}$$

to which must be added the two pure-gauge-field terms

$$H_{\text{electric}}=\sum_{\vec{r},\hat{n}}\frac{g^{2}}{2a}E^{2}(\vec{r},\hat{n})\,, \tag{2.30}$$

$$H_{\text{magnetic}}=-\sum_{\text{squares}}\frac{1}{ag^{2}}\,\mathrm{Tr}[U(1)U(2)U(3)U(4)]+\text{H.c.}\,, \tag{2.31}$$

where g is the coupling constnat, E is the electric part of the Yang-Mills field, and $\mathrm{Tr}[U(1)U(2)U(3)U(4)]$ is the trace around a unit lattice square.

Given the Hamiltonian in Eqs. (2.29)–(2.31), we are now ready to calculate various low-energy properties of quantum chromodynamics (QCD). At this stage in the program, however, we must make some working hypotheses to extract physical results from the lattice theory. We assume that conventional and lattice QCD agree if a goes to zero with g vanishing like $(\ln a)^{-1}$ (asymptotic freedom).[2] In addition, we assume that no phase transitions or critical points are encountered in varying g between ∞ and zero. High-order calculations of the mass spectrum of lattice QCD will eventually allow us to compute g as a function of a. Then we should explicitly confirm the asymptotic freedom of the theory and check that $g\to\infty$ as $a\to\infty$ (we hope). In the simpler Gross-Neveu model similar hypotheses were confirmed by explicit lattice calculations.[8]

III. THE STRONG-COUPLING VACUUM

The behavior of the theory for large g can be studied in strong-coupling perturbation theory. It is convenient to rescale our Hamiltonian defining

$$W=\frac{2a}{g^{2}}H\,. \tag{3.1}$$

Then

$$W=W_{e}+xW_{q}-2x^{2}W_{m}\,, \tag{3.2}$$

with

$$\begin{aligned}W_{e}&=\sum_{\vec{r},\hat{n}}E^{2}(\vec{r},\hat{n})\quad(\hat{n}=\hat{x},\hat{y},\hat{z}\text{ only})\\ W_{q}&=\sum_{\vec{r},\hat{n}}\chi^{\dagger}(\vec{r})U(\vec{r},\hat{n})\chi(\vec{r}+\hat{n})\eta(\hat{n})\\ &\qquad(\hat{n}=\hat{x},\hat{y},\hat{z},-\hat{x},-\hat{y},-\hat{z})\\ W_{m}&=-\sum_{\text{squares}}\mathrm{Tr}[U(1)U(2)U(3)U(4)]+\text{H.c.},\end{aligned} \tag{3.3}$$

where $x=1/g^{2}$. We now perturb about $x=0$. Thus to zeroth order only the "electric Yang-Mills" term W_{e} contributes, and the theory exists in a static limit. Hence, to zeroth order the ground state satisfies

$$W_{e}|0\rangle=0\,. \tag{3.4}$$

So, $|0\rangle$ is a state of zero flux. Since W_{e} is independent of the fermion degrees of freedom, there is a large degeneracy of ground states to zeroth order. We label the degenerate family of ground states $|0,\Psi\rangle$, where the zero indicates $E(\vec{r})=0$ and Ψ represents an arbitrary configuration of the fermion field.

We apply degenerate perturbation theory to determine the ground state for small x. Since $\langle 0,\Psi|W_{q}|0,\Psi\rangle=0$, the splitting between states of no flux but different fermion content does not occur until second order. We consider

$$x^{2}\left\langle 0,\Psi\left|W_{q}\frac{1}{\omega_{0}-W_{e}}W_{q}\right|0,\Psi\right\rangle, \tag{3.5}$$

where ω_{0} is the unperturbed energy of the ground state. It follows from Eq. (3.4) that $\omega_{0}=0$. Consider the possible intermediate states which can contribute to Eq. (3.5). W_{q} creates an excited link with electric flux satisfying $E^{2}=\frac{4}{3}$. It also creates a $q\bar{q}$ pair, but this costs no unperturbed energy so Eq. (3.5) reduces to

$$\begin{aligned}&-\tfrac{3}{4}x^{2}\langle 0,\Psi|W_{q}W_{q}|0,\Psi\rangle\\ &\quad=-\tfrac{3}{4}x^{2}\left\langle 0,\Psi\left|\left[\sum_{\vec{r},\hat{n}}\chi^{\dagger}(\vec{r})U(\vec{r},\hat{n})\right.\right.\right.\\ &\qquad\left.\left.\left.\times\chi(\vec{r}+\hat{n})\eta(\hat{n})\right]^{2}\right|0,\Psi\right\rangle.\end{aligned} \tag{3.6}$$

This expression can be simplified by recalling[9]

$$\langle 0,\Psi|U^{\dagger}_{ij}(\vec{r},\hat{n})U_{kl}(\vec{s},\hat{m})|0,\Psi\rangle=\tfrac{1}{3}\delta_{\vec{r},\vec{s}}\delta_{\hat{m},\hat{n}}\delta_{il}\delta_{jk}\,, \tag{3.7}$$

so that Eq. (3.6) becomes an effective Hamiltonian

involving only the fermion degrees of freedom

$$W_{\text{eff}} = \tfrac{1}{4} x^2 \sum_{\vec{r},\hat{n}} \rho(\vec{r})\rho(\vec{r}+\hat{n}) , \tag{3.8}$$

where

$$\rho(\vec{r}) = [\chi^\dagger(\vec{r}), \chi(\vec{r})] . \tag{3.9}$$

Thus, W_{eff} is the sum of nearest-neighbor couplings involving products of the local fermion numbers. The true ground state must minimize W_{eff} and be fluxless.

The space of fermion states is a tensor product with a finite-dimensional factor for each site. At each site we define a color-singlet state $|-3\rangle$ satisfying

$$\chi_i |-3\rangle = 0 , \tag{3.10}$$

where the index i denotes color. The notation -3 refers to the eigenvalue of ρ in this state

$$\rho|-3\rangle = -3|-3\rangle . \tag{3.11}$$

Applying $\chi_i^\dagger$ to $|-3\rangle$ creates a color triplet satisfying

$$\rho|-1,i\rangle = -1|-1,i\rangle . \tag{3.12}$$

Another application of $\chi_i^\dagger$ creates an antitriplet $|1,\bar{j}\rangle$,

$$\begin{aligned} &\tfrac{1}{2}\epsilon_{ijl}\chi_i^\dagger\chi_l^\dagger|-3\rangle = |1,\bar{j}\rangle , \\ &\rho|1,\bar{j}\rangle = |1,\bar{j}\rangle . \end{aligned} \tag{3.13}$$

Finally, a color singlet is obtained by applying $\chi_l^\dagger$ three times

$$\begin{aligned} &\tfrac{1}{6}\epsilon_{ijk}\chi_i^\dagger\chi_j^\dagger\chi_k^\dagger|-3\rangle = |3\rangle , \\ &\rho|3\rangle = 3|3\rangle . \end{aligned} \tag{3.14}$$

Returning to Eq. (3.8) it is evident that the lowest energy a link can have is $\frac{1}{4}(3)(-3)x^2 = \frac{9}{4}x^2$, which occurs when one end of the link has $\rho = 3$ and the other has $\rho = -3$. There are two states of the entire system which satisfy this criterion for every link. To define these states we will divide the sites into a pair of sublattices. The even (odd) sublattice consists of sites having $x+y+z$ even (odd). If we choose the state for which $\rho = +3$ on odd sites and -3 on even sites, every link will terminate on a $|3\rangle$ and a $|-3\rangle$. The only other state is obtained by interchanging odd and even sites. This twofold degeneracy is connected with chiral symmetry [see Eq. (2.18)] and is not lifted in higher order.

The vacuum is evidently both locally and globally color symmetric. This follows formally from the observation that the generator of local color-gauge transformations is[6]

$$G^\alpha(\vec{r}) = \sum_{\hat{n}} E^\alpha(\vec{r},n) + \chi^\dagger(\vec{r})\lambda^\alpha\chi(\vec{r}) , \tag{3.15}$$

and $G^\alpha(\vec{r})$ annihilates the vacuum since it is fluxless and the fermion states $|\pm 3\rangle$ are color singlets.

The vacuum is also invariant under the flavor-space transformation a, c, d, and e, since these take even (odd) sites into even (odd) sites. Only the chiral transformations b take even sites into odd sites. Therefore chiral symmetry is spontaneously broken by the effects of the interaction between gauge and quark fields. To better understand the nature of the breakdown let us consider the scalar operator $[\bar{q}, q]$. In the continuum theory,

$$\begin{aligned} [\bar{q}(\vec{r}), q(\vec{r})] = {} & [u_1^\dagger(\vec{r}), u_1(\vec{r})] + [u_2^\dagger(\vec{r}), u_2(\vec{r})] \\ & - [u_3^\dagger(\vec{r}), u_3(\vec{r})] - [u_4^\dagger(\vec{r}), u_4(\vec{r})] \\ & + (u \rightleftharpoons d) , \end{aligned} \tag{3.16}$$

which can be written in momentum space,

$$\bar{q}(\vec{r})q(\vec{r}) = \int u_1^\dagger(\vec{K})u_1(\vec{L})e^{i(\vec{K}-\vec{L})\cdot\vec{r}}d^3Kd^3L + \cdots . \tag{3.17}$$

Using $\vec{K} = \vec{k}/a$ and Eq. (2.10), we have

$$\begin{aligned} \bar{q}(\vec{r})q(\vec{r}) &= \int \phi^\dagger(\vec{k})\phi(\vec{l})e^{i(\vec{k}-\vec{l})\cdot\vec{r}} \\ &\quad \times e^{i\pi(x+y+z)}d^3kd^3l \\ &= \phi^\dagger(\vec{r})\phi(\vec{r})(-1)^{x+y+z} . \end{aligned} \tag{3.18}$$

Therefore,

$$\begin{aligned} [\bar{q}(\vec{r}), q(\vec{r})] &= [\chi^\dagger(\vec{r}), \chi(\vec{r})](-1)^{x+y+z} \\ &= \rho(\vec{r})(-1)^{x+y+z} . \end{aligned} \tag{3.19}$$

Since $\rho(\vec{r}) = \pm 3(-1)^{x+y+z}$ in the two degenerate ground states, we have in one vacuum,

$$\langle 0|[\bar{q}(\vec{r}), q(\vec{r})]|0\rangle = +3 , \tag{3.20a}$$

and in the other,

$$\langle 0|[\bar{q}(\vec{r}), q(\vec{r})]|0\rangle = -3 . \tag{3.20b}$$

These properties of the strongly coupled vacuum are important. It is generally believed that the real vacuum of the hadron world is both color and flavor symmetric, and that it spontaneously violates chiral invariance. Suppose for a moment that the strongly coupled theory behaved differently; e.g., some flavor symmetries might have been spontaneously broken. This would have been a disaster for our program since a phase transition would then separate the strongly coupled theory from the real hadron world. Then a smooth singularity-free extrapolation from $g = \infty$ to $g = 0$ would have been impossible.

Before turning to illustrative calculations, we shall consider a modification of the Hamiltonian

which is convenient when computing the meson spectrum. The modification of H renders the vacuum well determined by the unperturbed Hamiltonian itself. We place the following three demands on the new term. First, it must remove the undesired degeneracies in zeroth order. In this case the zeroth-order energy of nucleons and antinucleons is zero. Since degenerate perturbation theory is quite complicated when carried to high order, we want to add a static operator to H which lifts this degeneracy. Second, it must preserve the symmetries of the original Hamiltonian and again lead to a vacuum state which spontaneously breaks chiral symmetry. Third, it should have no effect on the continuum limit of the lattice theory; i.e., it should be an *irrelevant* operator.[14]

An operator with these properties is

$$W' = A \sum_{\vec{r},\hat{n}} [\rho(\vec{r})\rho(\vec{r}+\hat{n})+9] \ , \tag{3.21}$$

where A is a dimensionless (irrelevant) parameter. That W' satisfies the first and second conditions above should be clear. Condition 3 is, however, more subtle. W' is a four-fermion operator and, when written in terms of continuum variables with conventional units, it is multiplied by a coupling constant Ag^2a^2. Since the continuum limit is defined by $g^2 \to 0$, the four-fermion coupling tends to zero faster than a^2. Under these conditions a nonrenormalizable interaction is irrelevant.[14] In other words, although this interaction term exists on the finite lattice, it does not affect renormalized physical quantities in the continuum limit of the theory. In fact, cutoff Hamiltonians are always defined only up to the addition of irrelevant operators which are consistent with the symmetries of the physical system. Even if we wrote the lattice Hamiltonian without the W' term, we know that higher-order processes build up effective vertices which are four-fermion [Eq. (3.8) illustrates this point]. Adding W' to W is, therefore, just a convenience—in an adequate calculational scheme of the low-energy properties of W, the dependence on W' should disappear in the continuum limit. Later we shall study the dependence of our approximate results on the irrelevant parameter A. We shall find that in the $g \to 0$ limit the dependence on A becomes numerically insignificant for many low-energy quantities. This fact represents a useful check on the convergence of our approximate methods.

Now let us calculate the vacuum energy ω_0 in perturbation theory which incorporates W' in the unperturbed Hamiltonian.

In zeroth order clearly we have defined H such that

$$\omega_0^{(0)} = 0 \ . \tag{3.22}$$

There is no first-order or any odd-order contribution. To second order

$$\omega_0^{(2)} = x^2 \left\langle 0 \left| W_q \frac{1}{\omega_0^{(0)} - W_0} W_q \right| 0 \right\rangle , \tag{3.23}$$

where

$$W_0 = W_e + W' \ . \tag{3.24}$$

Diagrammatically we can represent this by Fig. 1. This figure is interpreted as follows. The lower horizontal line represents the action of W_e creating a $q\bar{q}$ pair on adjacent sites with a flux link between them. This amplitude is clearly $\eta(\hat{n})$. We then sample the energy of the intermediate state which is $\frac{4}{3} + 68A$ (dashed horizontal line). The term $68A$ is the $A\sum_{\vec{r},\hat{n}}[\rho(\vec{r})\rho(\vec{r}+\hat{n})+9]$ energy due to the presence of the q and $\bar{q}$ in the intermediate state. (Eleven links are affected by the $q\bar{q}$. Since $\rho = \pm 3$ on vacuum sites and $\rho = +1$ (-1) on sites with a q $(\bar{q})$, the eleven links contribute $(-3\times 10 - 1)A = -31A$. But in the vacuum the value of $A\sum[\rho(\vec{r})\rho(\vec{r}+\hat{n})+9]$ for these eleven links is $-9\times 11A = -99A$. The difference is $(-31+99)A = 68A$.) Finally the $q\bar{q}$ pair and their flux line are annihilated by the action of W_q with amplitude $\eta(-\hat{n})$. A factor of N (number of links on the lattice) is required since W_q can act on any link of the lattice. Thus

$$\omega_0^{(2)} = \frac{-3Nx^2}{\frac{4}{3} + 68A} \ , \tag{3.25}$$

where the factor of 3 comes from

$$\langle 0 | \chi(\vec{r}+\hat{n}) U^\dagger(\vec{r},\hat{n}) \chi(\vec{r}) \chi^\dagger(\vec{r}) U(\vec{r},\hat{n}) \chi(\vec{r}+\hat{n}) | 0 \rangle = 3 \ . \tag{3.26}$$

Now let us consider the two graphs of Fig. 2 which contribute to

$$\left\langle 0 \left| W_q \left(\frac{Q}{\omega_0^{(0)} - W_0} W_q \right)^3 \right| 0 \right\rangle , \tag{3.27}$$

where Q projects onto the subspace orthogonal to $|0\rangle$. This figure represents that contribution where

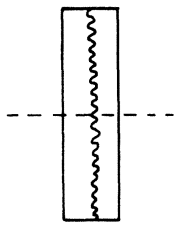

FIG. 1. Second-order vacuum graph. The horizontal dashed line indicates the energy denominator.

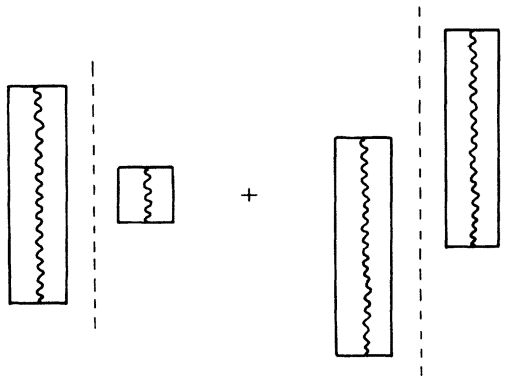

FIG. 2. Two fourth-order contributions to the vacuum energy. The dashed vertical line means that the quarks belonging to different connected pieces are *not* nearest neighbors.

W_q acts twice to produce $q\bar{q}$ pairs joined by flux links, but such that those quarks joined by different links are not on the same or adjacent sites. The contribution is therefore

$$\frac{-9\times 2\times N(N-57)}{2(\frac{4}{3}+68A)^3}x^4 . \tag{3.28}$$

The factor $(N-57)$ counts the number of places the second $q\bar{q}$ pair can be placed on the lattice such that neither of these fermions lie on the same sites or on sites adjacent to those occupied by the first $q\bar{q}$ pair. Next consider the contributions of Figs. 3(a) and 3(b). In Fig. 3(a) a quark on one link is on a site adjacent to an antiquark on the other. Hence W' acts to alter the central intermediate-state energy. In Fig. 3(b) the quarks on both links are adjacent to the antiquarks on the other link. The contribution of Fig. 3(a) is then

$$\frac{-9\times 2\times 42N}{(\frac{4}{3}+68A)^2(\frac{8}{3}+132A)}x^4 , \tag{3.29}$$

while that of Fig. 3(b) is

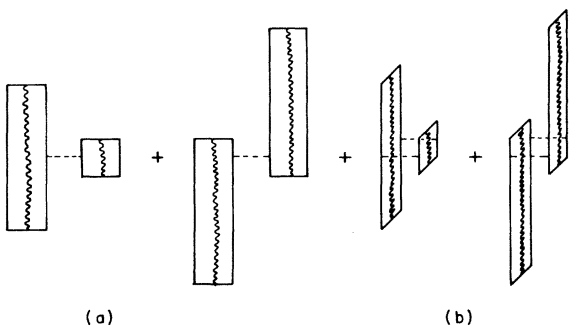

FIG. 3. (a) A fourth-order vacuum graph. The dashed horizontal line connects nearest-neighbor quarks. (b) The *two* dashed lines connect nearest neighbors.

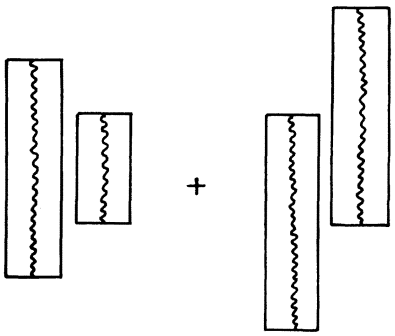

FIG. 4. Fourth-order vacuum graphs in which two quarks occupy one site.

$$\frac{-9\times 2\times 4N}{(\frac{4}{3}+68A)^2(\frac{8}{3}+128A)}x^4 . \tag{3.30}$$

Consider now the graphs of Fig. 4 where the second interaction produces a quark (antiquark) on the same lattice site as the first. Here the previous factor of 9 is reduced to 6 because the second quark on the middle lattice site can only be in one of two color states instead of three. Clearly these graphs yield a contribution

$$\frac{-6\times 2\times 10N}{(\frac{4}{3}+68A)^2(\frac{8}{3}+128A)}x^4 . \tag{3.31}$$

The last graph contributing is that of Fig. 5. Here explicit calculation of the contractions of U's and χ's yields a factor of 12. Antisymmetry of the quark wave functions tells us that the central flux state is in the $\bar{3}$ representation. Hence the contribution of this graph is

$$\frac{-12\times N}{(\frac{4}{3}+68A)^2(\frac{4}{3}+128A)}x^4 . \tag{3.32}$$

Next we should consider the contributions from

$$\left\langle 0\left| W_M \frac{1}{\omega_0^{(0)}-W_0} W_M\right| 0\right\rangle . \tag{3.33}$$

Here the first W_M creates a flux loop producing a state of energy $4\times\frac{4}{3}$. This loop is annihilated by the second W_M. Such a process is depicted in Fig. 6. The contribution is

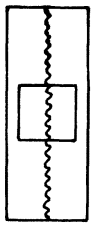

FIG. 5. A fourth-order vacuum graph occupying one link.

$$\frac{2N}{-4\times\frac{4}{3}}\,4x^4\,, \tag{3.34}$$

where the factor $2N$ is just the number of oriented squares on the lattice.

Finally, we must include a term

$$-\left\langle 0\left|W_q\,\frac{1}{\omega_0^{(0)}-W_0}\,W_q\right|0\right\rangle \times\left\langle 0\left|W_q\,\frac{1}{(\omega_0^{(0)}-W_0)^2}\,W_q\right|0\right\rangle \tag{3.35}$$

to compensate for using $\omega_0^{(0)}$ instead of ω_0 in the energy denominators.[15] This contribution is just

$$\frac{3Nx^2}{\frac{4}{3}+68A}\,\frac{3Nx^2}{(\frac{4}{3}+68A)^2}\,. \tag{3.36}$$

Collecting all these terms, our fourth-order vacuum energy is just

$$\omega_0^{(4)}=\left\{\frac{1}{(\frac{4}{3}+68A)^2}\times\left[\frac{513}{\frac{4}{3}+68A}-\frac{756}{\frac{8}{3}+132A}-\frac{204}{\frac{8}{3}+128A}\right]-\tfrac{3}{2}\right\}Nx^4\,.$$

Note that $\omega_0^{(4)}$ is proportional to N—the vacuum energy is an extensive quantity. Thus the N^2 dependence of Eq. (3.28) was precisely canceled by Eq. (3.36).

IV. THE LOW-MASS HADRON STATES

In the strong-coupling limit the lowest-lying $q\bar{q}$ states are those consisting of a quark and antiquark at opposite ends of a single link. If the quark is at $\vec{r}$ and the antiquark at $\vec{r}+\hat{n}$ we get a basis for such states $|\vec{r},\hat{n}\rangle$ as

$$|\vec{r},\hat{n}\rangle=\chi^\dagger(\vec{r})U(\vec{r},\hat{n})\chi(\vec{r}+\hat{n})|0\rangle\,. \tag{4.1}$$

For a zero-momentum state we require translational invariance, i.e., invariance under translating by two lattice sites in any direction. This still leaves us with the problem of determining the combination of $|\vec{r},\hat{n}\rangle$'s to use on the unit cube. For a given meson this "wave function" may be determined by its transformation properties under the discrete transformations of the theory. Alternatively, we can determine these states by taking the quark bilinear with the desired transformation properties and writing it in point-separated lattice form and applying it to the vacuum. For example, the pion state can be obtained (up to normalizations) by identifying

$$|\vec{\pi}\rangle\sim i\bar{\psi}\gamma_5\tfrac{1}{2}\vec{\tau}\psi|0\rangle\,.$$

This yields the strong-coupling wave functions for π, ρ, ω, σ, B, f_0, and A_1 listed below:

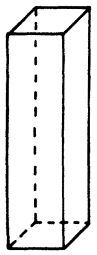

FIG. 6. A fourth-order pure gauge-invariant-excitation graph.

$$|\pi_0\rangle\sim i\bar{\psi}\gamma_5\tfrac{1}{2}\tau_3\psi|0\rangle\,, \tag{4.2a}$$

$$\sqrt{3}\,|\pi_0\rangle=i\Big[\sum_{\vec{r}}(-1)^x\chi^\dagger(\vec{r})U(\vec{r},\vec{n}_z)\chi(\vec{r}+\vec{n}_z)-\text{H.c.}\Big]|0\rangle\,,$$

$$|\omega_z\rangle\sim\psi^\dagger\alpha_z\psi|0\rangle\,, \tag{4.2b}$$

$$\sqrt{3}\,|\omega_z\rangle=i\Big[\sum_{\vec{r}}(-1)^y\chi^\dagger(\vec{r})U(\vec{r},\vec{n}_z)\chi(\vec{r}+\vec{n}_z)-\text{H.c.}\Big]|0\rangle\,,$$

$$|\rho_{3x}\rangle\sim\psi^\dagger\alpha_x\tfrac{1}{2}\tau_3\psi|0\rangle\,, \tag{4.2c}$$

$$\sqrt{3}\,|\rho_{3x}\rangle=\Big[\sum_{\vec{r}}(-1)^y\chi(\vec{r})U(\vec{r},\vec{n}_y)\chi(\vec{r}+\vec{n}_y)+\text{H.c.}\Big]|0\rangle\,,$$

$$|\sigma\rangle\sim i\bar{\psi}\not{\nabla}\psi|0\rangle\,, \tag{4.2d}$$

$$\sqrt{18}\,|\sigma\rangle=\sum_{\vec{r},\hat{n}}\chi^\dagger(\vec{r})U(\vec{r},\hat{n})\chi(\vec{r}+\hat{n})\eta(\hat{n})|0\rangle\,,$$

$$|B_{3z}\rangle\sim i\psi^\dagger\gamma_5\partial_z\tau_3\psi|0\rangle\,, \tag{4.2e}$$

$$\sqrt{3}\,|B_{3z}\rangle=\Big[\sum_{\vec{r}}(-1)^x\chi^\dagger(\vec{r})U(\vec{r},\vec{n}_z)\chi(\vec{r}+\vec{n}_z)+\text{H.c.}\Big]|0\rangle\,,$$

$$|f_{yy}\rangle\sim i\psi^\dagger(\alpha_z\partial_z+\alpha_x\partial_x-2\alpha_y\partial_y)\psi|0\rangle\,, \tag{4.2f}$$

$$2\sqrt{3}\,|f_{yy}\rangle=\Big[\sum_{\vec{r}}[(-1)^x\chi^\dagger(\vec{r})U(\vec{r},\vec{n}_z)\chi(\vec{r}+\vec{n}_z)+(-1)^z\chi^\dagger(\vec{r})U(\vec{r},\vec{n}_x)\chi(\vec{r}+\vec{n}_x)]+\text{H.c.}\Big]|0\rangle\,,$$

$$|A_{3z}\rangle\sim i\psi^\dagger(\alpha_x\partial_y-\alpha_y\partial_x)\tau_3\psi|0\rangle\,, \tag{4.2g}$$

$$\sqrt{6}\,|A_{3z}\rangle = \Big[\sum_{\vec{r}} [(-1)^y \chi^\dagger(\vec{r}) U(\vec{r}, \vec{n}_y)\chi(\vec{r}+\vec{n}_y) - (-1)^z \chi^\dagger(\vec{r}) U(\vec{r}, \vec{n}_x)\chi(\vec{r}+\vec{n}_x)] + \text{H.c.}\Big]|0\rangle \ .$$

Finally let us consider the nucleon. The lowest-energy three-quark state is obtained by putting three quarks on one lattice site. The correct combination for a spin-down neutron is

$$24\,|n\downarrow\rangle = \sum_{\vec{r}} [1 + (-1)^z + (-1)^{x+y} + (-1)^{x+y+z}] \times S(\vec{r})\epsilon_{ijk}\chi_i^\dagger(\vec{r})\chi_j^\dagger(\vec{r})\chi_k^\dagger(\vec{r})|0\rangle \ , \tag{4.3a}$$

the spin-up neutron,

$$24\,|n\uparrow\rangle = \sum_{\vec{r}} [1 - (-1)^z - (-1)^{x+y} + (-1)^{x+y+z}] \times S(\vec{r})\epsilon_{ijk}\chi_i^\dagger(\vec{r})\chi_j^\dagger(\vec{r})\chi_k^\dagger(\vec{r})|0\rangle \ , \tag{4.3b}$$

the spin-down proton,

$$24\,|p\downarrow\rangle = \sum_{\vec{r}} [-(-1)^x + (-1)^y - (-1)^{y+z} + (-1)^{x+z}] \times S(\vec{r})\epsilon_{ijk}\chi_i^\dagger(\vec{r})\chi_j^\dagger(\vec{r})\chi_k^\dagger(\vec{r})|0\rangle \ , \tag{4.3c}$$

and the spin-up proton,

$$24\,|p\uparrow\rangle = \sum_{\vec{r}} [-(-1)^x - (-1)^y - (-1)^{y+z} - (-1)^{x+z}] \times S(\vec{r})\epsilon_{ijk}\chi_i^\dagger(\vec{r})\chi_j^\dagger(\vec{r})\chi_k^\dagger(\vec{r})|0\rangle \ , \tag{4.3d}$$

where the quantity $S(\vec{r})$ was discussed in Sec. II.

Now we discuss the calculation of the energies of these states. In zeroth order (effectively $g = \infty$) the 1-link meson states all have "mass"

$$m_{1\ \text{link}} = \tfrac{4}{3} + 68A \ , \tag{4.4}$$

while the nucleon has "mass"

$$m_N = 108A \ . \tag{4.5}$$

Therefore, in this static limit (fixed and large a) the meson-to-nucleon mass ratios have strong dependence on the parameter A. Since states cannot propagate in this limit, all the single-link mesons have the same mass regardless of the character (e.g., s-wave or p-wave) of their continuum wave functions. The fourth-order calculations will cure these unphysical reflections of the static lattice approximation.

For large but not infinite g, we perturb in $x = 1/g^2$ as for the vacuum energy. We first illustrate such a calculation to order x^2 for the π, ρ, and ω. The other 1-link meson states behave similarly. First, however, we should observe that such a calculation should only be valid for $A > \frac{4}{3}/112$, since below this value, there exists an $N\bar{N}$ bound state with the same quantum numbers and lower energy at $g = \infty$. The point is that a state consisting of an N and an $\bar{N}$ separated by one link has static energy of $(9 \times 10)A - (-9 \times 10)A = 180A$. The $N\bar{N}$ state can be constructed to have the same quantum numbers as a "q-flux-$\bar{q}$" meson state which has a static energy of $\frac{4}{3} + 68A$. Only for $A > \frac{4}{3}/112$ will the q-flux-$\bar{q}$ state be less massive than the $N\bar{N}$ state in the static limit. For $A < \frac{4}{3}/112$ one should use the lighter $N\bar{N}$ state to find the mass of the lightest meson of those quantum numbers. In this article we will present nondegenerate-perturbation-theory calculations for $A > \frac{4}{3}/112$ and the results of a degenerate-perturbation-theory calculations at $A = \frac{4}{3}/112$.

Each component of π, ρ (six off-diagonal components), and ω consists of a linear combination of similarly directed links on the lattice. The phases [see Eq. (4.3)] are such that, if a link is annihilated by W_q and recreated but displaced longitudinally by a single unit, the amplitude acquires a negative sign. If the link is recreated after a transverse displacement by one link, the sign depends on whether it is a π, ρ, or ω. For π we get a positive sign for both transverse displacements, for ω we get a negative sign for both transverse displacements, while for the ρ we get a positive sign for one transverse direction and a negative for the other.

Now to the actual graphs which contribute to the second-order perturbation

$$\left\langle \left| W_q \frac{1}{\omega_1^{(0)} - W_0} W_q \right| \right\rangle . \tag{4.6}$$

The first is shown in Fig. 7. Here the single-link state is unaffected by the perturbation which merely produces and annihilates a $q\bar{q}$ pair with at-

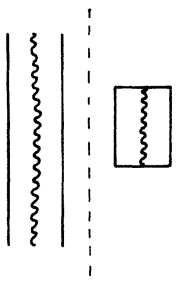

FIG. 7. A second-order contribution to the mass of a meson. The dashed line has the same meaning as in Fig. 2.

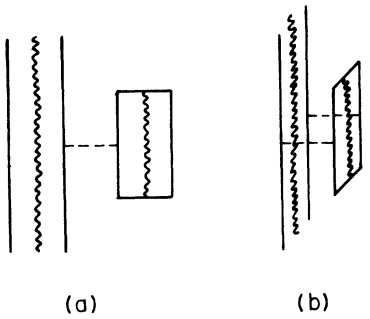

FIG. 8. Second-order contributions to a meson mass. The dashed lines connect nearest neighbors.

tendant flux link on sites that do not interact with the initial $q\bar{q}$ pair. The contribution is clearly

$$\frac{-3(N-57)}{\frac{4}{3}+68A} \tag{4.7}$$

for each of π, ρ, and ω.

Next we have those graphs in which the $q\bar{q}$ pair is produced such that W' gives an interaction between them and the single-link state. These are shown in Fig. 8. The contributions of Figs. 8(a) and 8(b) are

$$\frac{-3\times 42}{\frac{4}{3}+64A} \tag{4.8}$$

and

$$\frac{-3\times 4}{\frac{4}{3}+60A}\,, \tag{4.9}$$

respectively.

Now consider the case where the q (or $\bar{q}$) created by W_q lies on the same site as the q (or $\bar{q}$) of the initial state (Fig. 9). This gives a contribution

$$\frac{-2\times 10}{\frac{4}{3}+60A}\,. \tag{4.10}$$

Next we have that graph where W_q acts on the same link as the initial state, giving the graph of Fig. 10. The contribution is clearly

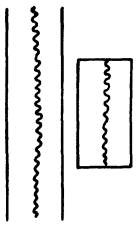

FIG. 9. A second-order graph in which one site is doubly occupied in the intermediate state.

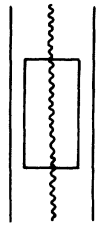

FIG. 10. A second-order single-link graph.

$$\frac{-4}{60A}\,. \tag{4.11}$$

We are now left with those graphs where the perturbation W_q annihilates the initial meson and recreates it (earlier or later), not usually on the same link. Clearly such graphs can distinguish π, ρ, and ω.

First we consider the case where the meson is created after annihilation (Fig. 11). Clearly all such contributions cancel since W_q cannot create a π, ρ, or ω out of the vacuum. Now we move on to graphs of Figs. 12, 13, 14, and 15. For the pion the contributions are

$$\frac{-3\times 3}{\frac{4}{3}+68A}\,,\ \frac{+3\times 6}{\frac{4}{3}+64A}\,,\ \frac{-3\times 4}{\frac{4}{3}+60A}\,,\ \text{and}\ \frac{2\times 2}{\frac{4}{3}+60A}\,, \tag{4.12}$$

respectively. For the ρ they give

$$\frac{3}{\frac{4}{3}+68A}\,,\ \frac{-3\times 2}{\frac{4}{3}+64A}\,,\ 0,\ \text{and}\ \frac{2\times 2}{\frac{4}{3}+60A}\,, \tag{4.13}$$

respectively. Finally, for the ω we have

$$\frac{3\times 5}{\frac{4}{3}+68A}\,,\ \frac{-3\times 10}{\frac{4}{3}+64A}\,,\ \frac{3\times 4}{\frac{4}{3}+60A}\,,\ \text{and}\ \frac{2\times 2}{\frac{4}{3}+60A}\,. \tag{4.14}$$

Thus the second-order contribution to the ω energy

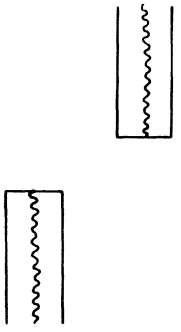

FIG. 11. A second-order graph in which the meson can propagate. Summing the later vertex over the entire lattice gives zero for the π, ρ, and ω.

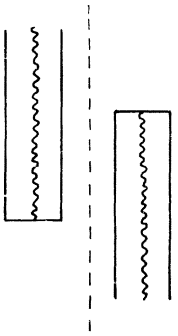

FIG. 12. A different time ordering of the graph in Fig. 11. The vertical dashed line has the usual interpretation.

for π, ρ, and ω is

$$\omega_\pi^{(2)} = \frac{162}{\frac{4}{3}+68A} - \frac{108}{\frac{4}{3}+64A} - \frac{40}{\frac{4}{3}+60A} - \frac{4}{60A}\,, \tag{4.15a}$$

$$\omega_\rho^{(2)} = \frac{174}{\frac{4}{3}+68A} - \frac{132}{\frac{4}{3}+64A} - \frac{28}{\frac{4}{3}+60A} - \frac{4}{60A}\,, \tag{4.15b}$$

$$\omega_\omega^{(2)} = \frac{186}{\frac{4}{3}+68A} - \frac{156}{\frac{4}{3}+64A} - \frac{16}{\frac{4}{3}+60A} - \frac{4}{60A} \tag{4.15c}$$

after subtracting the vacuum energy.

As a further example we look at the second-order contribution to the nucleon. There are only two types of graph which contribute. The first is depicted in Fig. 16. Its contribution is clearly

$$\frac{-3(N-36)}{\frac{4}{3}+68A}\,. \tag{4.16}$$

The other graph is that of Fig. 17 which gives

$$\frac{-3\times 30}{\frac{4}{3}+56A}\,. \tag{4.17}$$

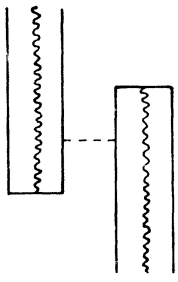

FIG. 13. The meson propagates in second order, and two quarks in the intermediate state are nearest neighbors.

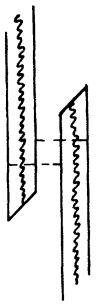

FIG. 14. All quarks in the intermediate state are nearest neighbors.

Thus the second-order contribution to the nucleon ω energy is

$$\omega_N^{(2)} = \left(\frac{108}{\frac{4}{3}+68A} - \frac{90}{\frac{4}{3}+56A}\right)x^2\,. \tag{4.18}$$

These results and those for the other mesons have been calculated to fourth order. Results for the series for ω_1 calculated to fourth order are given below for the single-link mesons for the value $A = \frac{4}{3}/112$, where we had to do degenerate perturbation theory for the $q\bar{q}$ and $N\bar{N}$ states.

$$\omega_\pi = 2.143 - 3.516x^2 + 66.173x^4\,, \tag{4.19a}$$

$$\omega_\omega = 2.143 - 3.507x^2 + 66.435x^4\,, \tag{4.19b}$$

$$\omega_\rho = 2.143 - 3.512x^2 + 66.222x^4\,, \tag{4.19c}$$

$$\omega_\sigma = 2.143 - 0.880x^2 + 48.134x^4\,, \tag{4.19d}$$

$$\omega_B = 2.143 - 1.821x^2 + 55.891x^4\,, \tag{4.19e}$$

$$\omega_f = 2.143 - 3.516x^2 + 167.315x^4\,, \tag{4.19f}$$

$$\omega_{A_1} = 2.143 - 9.88x^2 + 49.109x^4\,. \tag{4.19g}$$

The nucleon series for this value of A is

$$\omega_N = 1.296 + 5.368x^2 - 15.029x^4\,. \tag{4.20}$$

The series results for more general values of A are presented in Tables I and II.

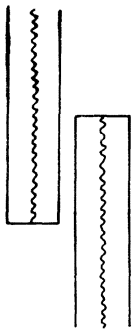

FIG. 15. Two quarks in the intermediate state occupy a single site.

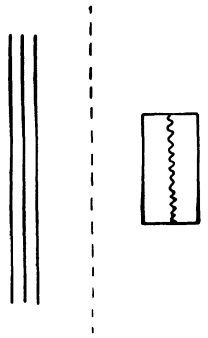

FIG. 16. A second-order contribution to the nucleon mass.

V. MASS RATIOS IN THE CONTINUUM LIMIT

The series given in the preceding section are only valid for g^2 large. Since from renormalization-group arguments for an asymptotically free theory

$$g^2 = \frac{-c}{\ln a} \tag{5.1}$$

for small a, then clearly the above series are valid only for large lattice spacings. Hence we need some method of continuing our series to $g=0$, i.e., $x=\infty$, which is the continuum limit.

First we note that since we are really interested in eigenvalues of

$$H = \frac{g^2}{2a} W \tag{5.2}$$

all our series must be multiplied by $g^2/2a = e^{+cx}/x$. This makes continuation difficult. However, if we consider only mass ratios these factors cancel and the result can be expanded as a power series in x.

We now use the method of Padé approximants, long used with success in statistical mechanics, to continue these series to large x. We take our polynomial (to this order quadratic) in $y=x^2$ and write it in the form

$$\frac{1+\alpha y}{1+\beta y}\ , \tag{5.3}$$

where α and β are determined by expanding this to order y^2 and equating coefficients. We can now take the continuum $y \to \infty$ limit yielding α/β.

We now present the results obtained in this manner for the ratios m/m_N for the single-link mesons

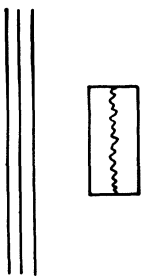

FIG. 17. One quark of the loop is a nearest neighbor of the nucleon.

TABLE I. Expansion coefficients and continuum masses measured relative to the nucleon for various hadrons at difference choices of the irrelevant parameter ξ. The expansion coefficients occur in the expressions $\omega_i = \omega_i^{(0)} + \omega_i^{(2)}x^2 + \omega_i^{(4)}x^4$, where i denotes the hadron of interest. At $\xi = 0.61$ degenerate perturbation theory must be applied. Nondegenerate perturbation theory gives the results at $\xi = 1.02$ and 1.43. Quasidegenerate perturbation theory lowers the $\xi = 1.02$ results to those shown in the graphs. At $\xi = 1.43$ the nondegenerate results are very accurate.

Hadron	ξ	$\omega^{(0)}$	$\omega^{(2)}$	$\omega^{(4)}$	m/m_N
ρ	0.61	2.143	−3.512	66.222	0.822
	1.02	2.693	−0.292	12.483	0.894
	1.43	3.237	−0.161	4.075	0.824
ω	0.61	2.143	−3.507	66.435	0.824
π	0.61	2.143	−3.516	66.173	0.821
σ	0.61	2.143	−0.880	41.963	0.989
	1.02	2.693	1.955	6.994	1.11
	1.43	3.237	1.391	1.132	0.995
B	0.61	2.143	−1.821	55.891	0.95
	1.02	2.693	1.560	11.109	1.10
	1.43	3.237	1.433	3.623	1.02
f	0.61	2.143	−3.516	165.708	1.17
	1.02	2.693	−0.301	76.698	1.14
	1.43	3.237	−0.171	41.436	1.02
A_1	0.61	2.143	−0.988	47.502	1.00
	1.02	2.693	2.303	8.541	1.15
	1.43	3.237	1.943	1.943	1.07
Nucleon	0.61	1.296	5.368	−15.029	...
	1.02	2.160	3.414	−6.015	...
	1.43	3.024	2.341	−3.194	...

TABLE II. Expansion coefficients and the continuum value of g_A for various choices of ξ.

ξ	$g_A^{(0)}$	$g_A^{(2)}$	$g_A^{(4)}$	g_A
0	3.00	−14.58	178.89	1.81
0.31	3.00	−7.22	55.02	2.10
0.61	3.00	−4.42	15.76	2.04
0.92	3.00	−2.96	6.47	1.91
1.22	3.00	−2.11	3.62	1.70
1.53	3.00	−1.58	2.49	1.31

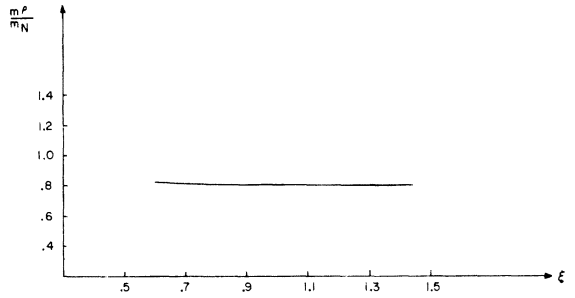

FIG. 18. The continuum ratio m^ρ/m_N ([1, 1] Padé of the mass ratio, x has passed to infinity) vs the irrelevant parameter ξ.

at $A = \frac{4}{3}/112$,

$$m^\rho/m_N = 0.822 \ , \tag{5.4a}$$

$$m^\omega/m_N = 0.824 \ , \tag{5.4b}$$

$$m^\pi/m_N = 0.820 \ , \tag{5.4c}$$

$$m^\sigma/m_N = 1.01 \ , \tag{5.4d}$$

$$m^B/m_N = 0.95 \ , \tag{5.4e}$$

$$m^f/m_N = 1.17 \ , \tag{5.4f}$$

$$m^{A_1}/m_N = 1.00 \ . \tag{5.4g}$$

The results for more general A are given in the tables and the graphs of Figs. 18, 19, and 20.

We discuss briefly several interesting features of these calculations. For each mass ratio considered here, the [1, 1] Padé approximant exists with positive values for α and β. Therefore, an extrapolation from $y = 0$ to $y = \infty$ is singularity-free in this approximation. This result gives us some confidence that the only phase of QCD is one which is strongly coupled at large distances. Of course, higher-order calculations are essential to *really* argue this point.

Observe from the tables that the expansion coefficients for ω_{meson} and ω_N depend strongly on the irrelevant parameter A, while the mass ratios do not. A meaningful measure of the size of A is contained in the parameter $\xi = 68A/\frac{4}{3}$, which parametrizes the graphs. ξ measures the amount of irrelevant energy on the scale of flux energy $(\frac{4}{3})$ in the unperturbed meson states. In the graphs ξ varies from 0.61 to 1.43 (more than a factor of 2) and m^ρ/m_N, for example, varies only a few percent over this range. This is a good indication that the calculational and extrapolation method is respecting some general field-theoretic principles. Note that the p-wave meson-to-nucleon mass ratios have more dependence on ξ. Since p-wave wave functions have more spatial variation than s-wave wave functions, this trend in the results is not unexpected. Higher-order calculations will be necessary to approximate accurately the wave functions of excited states using lattice methods. The fact that the Taylor-series coefficients depend significantly on A while the mass ratios do not can be understood in the following way. Since the irrelevant operator W' is generated naturally by perturbative effects in the theory with nonzero lattice spacing, the presence of W' in the original W energy expression can be compensated for by a rescaling of the lattice spacing. Such a rescaling, however, can be compensated for by a multiplicative change in the lattice coupling constant $g(a)$. Since $g(a)$ is taken to zero in the continuum limit, a multiplicative change in $g(a)$ must have no effect on the calculation of mass ratios. Therefore, the large changes in the coefficients presented in the tables for various values of A can, to good approximation, be removed by rescaling the expansion parameter x.

In Eq. (5.4) we measure the meson masses relative to the nucleon mass in every case. These ratios are expected to be more reliable at low orders than ratios involving two mesons. The reason for this is that all the mesons are degenerate in zeroth order so small differences of second and fourth Taylor-series coefficients control the [1, 1] Padé approximants, and a considerable amount of information in the series is lost. When more Taylor-series coefficients are

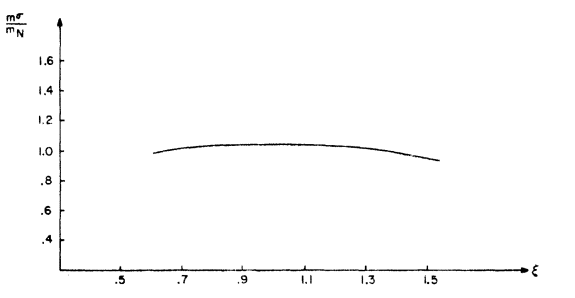

FIG. 19. Same as Fig. 18, except for m^σ/m_N.

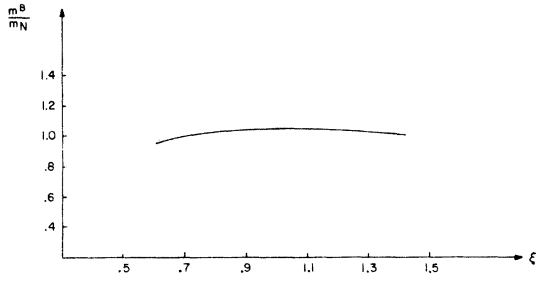

FIG. 20. Same as Fig. 19, except for m^B/m_N.

computed, however, all the ratio calculations should be consistent. Even at fourth order the ρ, σ, and N series are consistent in the sense that the Padé approximants for m^ρ/m_N, m^σ/m_N, and m^ρ/m^σ all exist and give almost (within 20%) the same estimates of the particle masses.

It is clear that, with the exception of the pion, these mass ratios are encouraging. The fact that the π-ρ splitting is so tiny can be traced, we believe, to the lack of spin-spin forces in the first four orders of $1/g^2$ perturbation theory. A survey of graphs shows that magnetic field effects, loops of flux, are just not important through this order. However, at sixth and eighth order such effects appear to be important, so we hope to do better in the near future. Related to this problem is the fact that lattice-fermion methods do not allow one to formulate the theory with *continuous* chiral symmetry for $a \neq 0$—the fermion method discussed here has only discrete pieces of the flavor symmetries for $a \neq 0$. In the continuum limit the asymptotic freedom of the theory assures us that the continuous symmetries are restored when $a \to 0$ since they are present in the long wavelengths of the lattice free fields. According to the Goldstone theorem, it is continuous chiral symmetry and the presence of an order parameter $\langle \bar{q}q \rangle \neq 0$ (spontaneous symmetry breaking) which guarantee a massless pion triplet. If continuous chiral symmetry is retrieved very slowly order by order in $1/g^2$ perturbation theory, then our calculational scheme may be impractical.

VI. CALCULATION OF g_A

Static and near-static properties of hadrons are also accessible in the strong-coupling calculational scheme discussed here. Consider the axial charge of the nucleon g_A,

$$g_A = \left\langle N \left| \int \bar{\psi} \gamma_z \gamma_5 \tau_3 \psi \, d^3x \right| N \right\rangle . \tag{6.1}$$

Our first task is to write the operator,

$$\begin{aligned} \mathcal{O}_A &= \int \bar{\psi} \gamma_z \gamma_5 \tau_3 \psi \, d^3x \\ &= \int J^5_{z,3} d^3x , \end{aligned} \tag{6.2}$$

in terms of the lattice fermions. Using the methods of Sec. II, we compute

$$\mathcal{O}_A = \sum_{\vec{r}} (-1)^x \chi^\dagger(\vec{r}) \chi(\vec{r}) . \tag{6.3}$$

Comparing this to the mass operator,

$$\int \bar{\psi}\psi \, dx \to \sum_{\vec{r}} (-1)^{x+z} \chi^\dagger(\vec{r}) \chi(\vec{r}) , \tag{6.4}$$

we can formulate a useful rule for calculating Eq. (6.1): Quarks (or antiquarks) at z-even sites contribute $+1$ to g_A, and quarks (or antiquarks) at z-odd sites contribute -1 to g_A.

A convenient way to organize the calculation of g_A is to apply the Feynman-Hellmann theorem.[16] We add to W_e the operator $\lambda \mathcal{O}_A$, where λ is a useful dimensionless parameter, and treat the sum as the unperturbed W. Then perturbation theory in x is done in a conventional fashion. The energy denominators now have λ dependence. If we calculate the $\omega_N(\lambda)$ now, then[16]

$$g_A = \langle N | \mathcal{O}_A | N \rangle = \frac{\partial}{\partial \lambda} \omega_N(\lambda) \Big|_{\lambda = 0} . \tag{6.5}$$

Now we shall sketch the calculation of $\omega_N(\lambda)$ through $O(x^2)$. In zeroth order the only graph which contributes is shown in Fig. 21,

$$\omega_N^{(0)}(\lambda) = 3\lambda . \tag{6.6}$$

So, the zeroth-order approximation to g_A is

$$g_a^{(0)} = 3 . \tag{6.7}$$

We shall see below that strong-coupling perturbation theory improves this result considerably.

The graphs which contribute to $\omega_N(\lambda)$ in second order are shown in Figs. 16 and 17. The λ-dependent terms coming from Fig. 16 are, after the vacuum subtraction,

$$\frac{24}{\frac{4}{3} + 68 - 2\lambda} + \frac{48}{\frac{4}{3} + 68A + 2\lambda} , \tag{6.8a}$$

and from Fig. 17,

$$- \frac{24}{\frac{4}{3} + 56A - 2\lambda} - \frac{36}{\frac{4}{3} + 56A + 2\lambda} . \tag{6.8b}$$

Equations (6.8a) and (6.8b) sum to $\omega_N^{(2)}(\lambda)$. Differentiating with respect to λ we obtain

$$g_A^{(2)} = - \frac{48}{(\frac{4}{3} + 68A)^2} + \frac{24}{(\frac{4}{3} + 56A)^2} . \tag{6.9}$$

The fourth-order calculation proceeds straightforwardly. The results are shown in the appropriate table and the graph of g_A vs the irrelevant parameter ξ (Fig. 22).

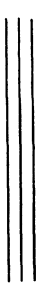

FIG. 21. The zeroth-order nucleon.

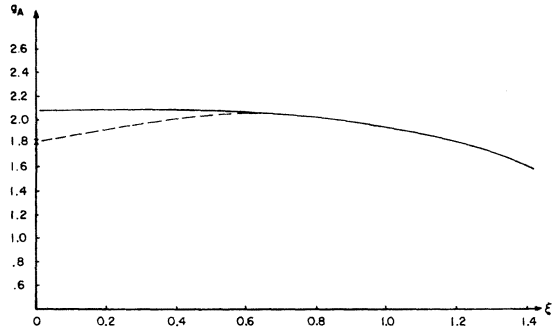

FIG. 22. The continuum g_A vs ξ. The x at $\xi=0$ is the result of a degenerate-perturbation-theory calculation. The solid line is a nondegenerate-perturbation-theory calculation. The dashed line is an educated guess at a quasidegenerate-perturbation-theory calculation which should smoothly connect the two calculations actually done in detail and discussed in the text.

Finally, g_A was calculated at $\xi=0$ using degenerate perturbation theory. Setting $A=0$ allows $N\bar{N}$ pairs to mix with the single nucleon state in $O(x^3)$, and these effects can be computed using standard methods. The resulting expansion for g_A reads

$$g_A = 3 - 14.58x^2 + 178.89x^4 \ . \tag{6.10}$$

Forming the $[1,1]$ Padé approximant, we have

$$g_A = 3\,\frac{1+7.410x^2}{1+12.270x^2} \xrightarrow[x\to\infty]{} 1.81 \ . \tag{6.11}$$

We conclude that strong-coupling perturbation theory improves g_A significantly from its static value. It will be interesting to see how closely the eighth-order calculation comes to the experimental value of 1.24 ± 0.02.

VII. DISCUSSION

We have performed a perturbative calculation of the masses of the nucleon and low-lying mesons on a spatial lattice in the strong-coupling region. Since we assume that the continuum limit obtains without any phase transitions, we analytically continue the series using Padé approximants, limiting ourselves to mass ratios where the known singularities of the $a=0$ limit cancel.

With the exception of the pion, which is nearly degenerate with the ρ in mass, the results are in good agreement with the measured masses. The difficulty with the pion is most easily understood by noting that it is only the A term which we added by hand that splits the π, ρ, and ω to this order. Natural mass splitting of this system relies on "magnetic Yang-Mills" and induced "magnetic Yang-Mills" flux terms and arises first at sixth order.

The value of g_A, i.e., $g_A=1.81$, is not very good although the fact that it is well below the zeroth-order value of 3 is encouraging. However, it is probably to be expected that g_A will not settle down to a better value until the pion mass improves.

Thus we see that our results, while encouraging, need extending to higher orders. This requires computerization of the graph counting and calculation and has already been started. Alternatively, one can try to start with a lattice Hamiltonian, constructed using renormalization-group techniques, which more closely represents the continuum theory. Work on this approach is also in progress. Calculations have begun which use Hamiltonians having significant π-ρ splitting in $O(x^2)$.

ACKNOWLEDGMENTS

The author thank K. G. Wilson for suggestions, guidance, and criticism. J. K. thanks Tel Aviv University for its warm hospitality and the Israel Commision for Basic Research for partial financial support. D. K. Sinclair and L. Susskind thank Cornell University for its hospitality and partial financial support during various stages of this work.

*Work supported in part by the Israel Commission for Basic Research.

†Work supported in part by the National Science Foundation under Grant No. GP-38863. Permanent address: Belfer Graduate School of Science, Yeshiva University, New York, N.Y. 10033.

‡Work supported in part by the Alfred P. Sloan Foundation and in part by the National Science Foundation.

§Work supported in part by a grant from I.B.M.

‖Work supported by the U.K. Science Research Council.

[1]The term "quantum chromodynamics" has been suggested by M. Gell-Mann. Advantages of this theory over previous field-theoretic formulations of the quark model were pointed out by H. Fritzsch, M. Gell-Mann, and H. Leutwyler, Phys. Lett. 47B, 365 (1973).

[2]G. 't Hooft, Marseilles conference on gauge theories, 1972 (unpublished); H. D. Politzer, Phys. Rev. Lett. 30, 1346 (1973); D. J. Gross and F. Wilczek, *ibid.* 30, 1343 (1973).

[3]See, for example, the third entry in Ref. 2 and S. Weinberg, Phys. Rev. Lett. 11, 255 (1964).

[4]K. G. Wilson, Phys. Rev. D 10, 2445 (1974).

[5]A. M. Polyakov (unpublished); and Phys. Lett. 59B, 82 (1975).

[6]J. Kogut and Leonard Susskind, Phys. Rev. D 11, 395 (1975); T. Banks, L. Susskind, and J. Kogut, *ibid.* 13, 1043 (1976).

[7]A. Carroll, J. Kogut, D. K. Sinclair, and L. Susskind,

Phys. Rev. D 13, 2270 (1976).
[8]J. Shigemitsu and S. Elitzur, Phys. Rev. D 14, 1988 (1976).
[9]J. Kogut, D. K. Sinclair, and Leonard Susskind, Nucl. Phys. B114, 199 (1976).
[10]P. W. Higgs, Phys. Lett. 12, 132 (1964); Phys. Rev. Lett. 13, 508 (1964); Phys. Rev. 145, 1156 (1966); F. Englert and R. Brout, Phys. Rev. Lett. 13, 321 (1964); G. S. Guralnik, C. R. Hagen, and T. W. B. Kibble, *ibid.* 13, 585 (1964); T. W. B. Kibble, Phys. Rev. 155, 1554 (1967).
[11]The computer calculations are being done by A. Carroll, G. Frye, R. Fredrickson, and others.
[12]L. Susskind, Phys. Rev. D (to be published).
[13]See the "Search and Discovery" section of Phys. Today 29, No. 7 (1976).
[14]K. G. Wilson and J. Kogut, Phys. Rep. 12C, 75 (1974).
[15]The relation between Wigner-Brillouin and Rayleigh-Schrödinger perturbation theory is discussed in Ref. 7.
[16]See E. Merzbacher, *Quantum Mechanics* (Wiley, New York, 1970), 2nd edition, Chap. 17, Sec. 8., for a discussion of the Feynman-Hellmann theorem.